PHYSICAL REVIEW A VOLUME 22, NUMBER 5 NOVEMBER 1980

Quasimolecular inner-shell charge-transfer cross sections for light projectiles in solids

J. D. Garcia* and R. J. Fortner
Lawrence Livermore Laboratory, Livermore, California 94550

H. C. Werner, D. Schneider, N. Stolterfoht, and D. Ridders
Hahn Meitner Institut für Kernforschung, West Germany

(Received 11 January 1980)

K-shell vacancy fractions have been measured for B, C, N, O, and Ar projectiles traversing thin carbon foils. The equilibrium vacancy fractions were determined by measuring Auger electron yields from the projectiles emerging from the foils. Projectile energies ranged from 50 to 500 keV. The fractions increase as energy increases, up to saturation values. The measurements are interpreted in terms of vacancy creation and filling events, using previously measured cross sections and vacancy sharing ratios. Collisional vacancy filling cross sections for projectile-carbon atom collisions are extracted, and the mechanisms responsible for saturation are delineated. These cross sections are compared to available theoretical estimates and are found to be much larger than those predicted by modified Brinkman-Kramers theory. This is attributed to quasimolecule-formation effects. Tentative values for dynamical projectile vacancy lifetimes are obtained.

Although the excitation states of projectiles moving through solids have been of interest for several decades,[1-4] direct information concerning them has been scarce. It has been recently recognized, however, that measurements of Auger electron and x-ray emissions by the projectile provide quantitative information about some aspects of these excitation states. Studies[5-13] of these emissions have provided a framework for understanding the inner-shell excitations of the moving projectiles and the way in which these approach their equilibrium values as the projectile moves through the solid.

In this paper we report measurements of absolute Auger electron yields from light projectiles that have traversed thin carbon foils. The foil thicknesses were chosen to ensure that the fraction of projectiles having an inner-shell vacancy had reached its equilibrium value. As the projectile energies were varied from 50 to 500 keV, these fractions were observed to increase up to saturation values. For the projectiles chosen, the single-collision inner-shell vacancy-production cross sections and vacancy-sharing ratios for collisions with carbon atoms have been previously measured.[14] Analysis of the present data using this information has yielded inner-shell charge-transfer cross sections at energies which are small enough to show quasimolecular effects rather spectacularly. These cross sections are compared to available theoretical estimates. Tentative values for the lifetimes of the projectile vacancy states are also obtained.

The experimental procedure has been described in detail elsewhere[7,14]; only a brief sketch is given here. B^+, C^+, N^+, O^+, and Ar^+ ions were accelerated with a model AN Van de Graaff accelerator. The energies were varied between 50 and 500 keV, and charge state and energy determinations were made using a calibrated analyzing magnet. Energy determination accuracy ranged from 2% at the highest to 5% at the lowest energy used. After leaving the magnet, the beam was focused by a quadrupole magnet, entered the target chamber through a series of collimators, passed through a thin carbon foil, and was collected in a biased Faraday cup. Beam current was kept low (5–20 nA) to avoid foil damage. The target area was viewed by a rotatable electrostatic parallel-plate analyzer (90° angle). The resolution of the electron analyzer was 2.6% full width at half maximum (FWHM). This simultaneous measurement of the beam flux and electrons at a given angle θ relative to the beam direction results in an absolute determination of the differential secondary electron production probability.

The carbon foil thicknesses were chosen to insure that equilibrium values of the inner-shell vacancy fractions were measured. This was checked by varying the foil thickness. For all projectiles except oxygen, foil thicknesses of 3, 5, and 10 $\mu g/cm^2$ produced results which were identical to each other within statistical error, for the same final energy. The oxygen case is discussed below.

The resultant secondary electron spectra showed features identifiable as projectile and target Auger electrons superposed on a continuous background which decreased monotonically as secondary electron energy increased.[7,14] The background continuum was fitted at points on either side of the Auger peaks and subtracted. The resultant projectile Auger peaks were measured at various

angles relative to the beam direction and were found to be isotropic in the projectile rest frame. The expected Doppler effect on the Auger electron energies due to the motion of the emitter was observed, and this was used to separate target and projectile Auger electrons in most cases. Because of the measured isotropy of the Auger peaks, we were able to integrate the spectrum over energy and angle to obtain absolute Auger yields per projectile. The spectra showed negligible (≪10%) effects due to emission of projectile electrons while the projectile was still in the foil—emission occurred predominantly after emergence from the foil. For carbon target Auger electrons, on the other hand, the low-energy side of the spectrum was markedly enhanced, in some cases so much that no distinct peak was evident.

In the case of oxygen projectiles, the spectra showed projectile oxygen Auger electrons, carbon Auger electrons, and a clear peak which *was not Doppler shifted*, attributable to oxygen target Auger electrons. We also made measurements of secondary electrons emitted at angles greater than 90° relative to the beam direction (i.e., in front of the foil). At these angles we saw no evidence of Doppler-shifted oxygen projectile Auger electrons (as expected, since these electrons are stopped by the foil), but the unshifted peak was observed. We estimated on the basis of these measurements that the carbon foils had an oxygen impurity amounting to about 5% of the carbon atomic density. This number is quite uncertain (~a factor of 2), but these results present substantial difficulty in interpreting the results using oxygen projectiles, as discussed below.

The yield per projectile ion accurately represents the *equilibrium* vacancy fraction for the projectile, i.e., the fraction of projectiles having an inner-shell vacancy. For these projectiles at these energies, the filling of vacancies accompanied by emission of an x-ray is negligible compared to Auger electron emission. These vacancy fractions are presented in Fig. 1, as functions of the projectile energy after exising the foil. We estimate a relative uncertainty of 20% and an absolute uncertainty of 30% for energies above 100 keV, 30% and 40%, respectively, for energies of 100 keV or less.

It can be seen from Fig. 1 that for Ar, B, C, and N projectiles, the vacancy fractions approach a saturation value as a function of projectile energy.

Our understanding of the reasons for this saturation is based on the fact that these measurements correspond to equilibrium—i.e., steady state—vacancy fractions for the projectiles. For

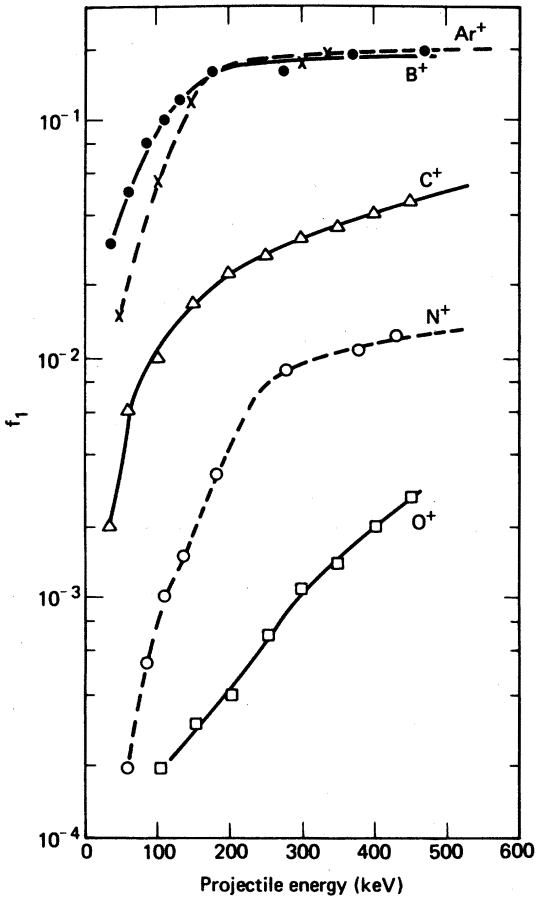

FIG. 1. Steady-state K-vacancy fractions for projectiles moving through carbon foils as functions of exit projectile energy: filled circles, boron; crosses, argon; triangles, carbon; open circles, nitrogen; squares, oxygen. The lines are guides to the eye.

this situation, and assuming that the K-shell levels of the projectiles remain well defined in the solid, we can write rate equations for the fraction of ions having an inner-shell vacancy f_1:

$$\frac{df_1}{dx} = N\sigma_{01}f_0 - N\sigma_{10}f_1 - \frac{f_1}{v\tau}, \qquad (1)$$

$$f_0 + f_1 = 1,$$

where f_0 is the fraction of the projectiles having no inner-shell vacancies, N is the density of foil atoms, σ_{01} is the cross section for vacancy production in the projectile in projectile ion-carbon atom collisions, σ_{10} is the collisional vacancy-filling cross section, τ is the vacancy lifetime for spontaneous decay (possible velocity dependent), v is the projectile speed, and x is the distance traveled in the foil. At steady state, $df/dx \equiv 0$.

The vacancy production cross section σ_{01} for these projectiles have been measured[14] for carbon atoms in gas targets. The steady-state equations

can be written as

$$\sigma_{01} f_0/f_1 = \sigma_{10} + 1/N v \tau , \tag{2}$$

that is, the unknown charge-transfer cross section and the effective cross section associated with spontaneous decay are related to the product of the known vacancy production cross section and the ratio of the measured vacancy fractions. These are shown in Fig. 2(a). Since both terms on the right-hand side of (2) are energy dependent, it is difficult to separate their effects.

We can go one step further in understanding the saturation of the vacancy fractions by assuming that the vacancy-filling cross sections can be understood in terms of the quasimolecule formed by the collision partners. This model has been successfully applied to vacancy production[14,15] and it is commonly accepted as the most applicable model for dealing with K-shell electron promotions. If we restrict our attention to the K shells of the carbon and projectile atoms, this model describes the vacancy filling as a transfer of an electron from the K shell of the carbon atom to the vacancy in the projectile K shell, occurring at relatively large (~1 a.u.) distances due to radial coupling of the 1σ and 2σ orbitals during the collision. According to this restricted two-level description of the process, it is the inverse process to vacancy production and the cross section is given by a (energy-independent) geometrical factor,[16] πR_x^2, multiplied by the two-pass probability for sharing the vacancy between the two orbitals.

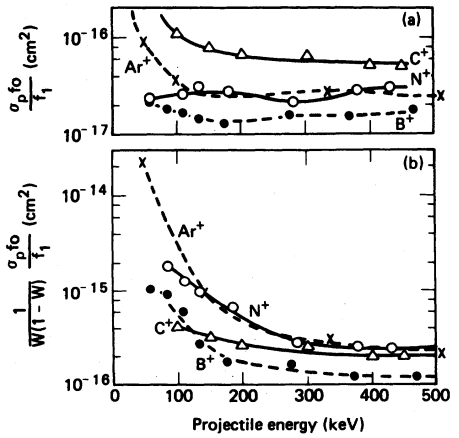

FIG. 2. Reduced vacancy production cross sections. (a) Vacancy-production cross sections, σ_p, multiplied by the ratio of projectiles having no vacancies to those having a vacancy, as functions of exit projectile energy. (b) Geometrical factors. The quantities $[1/W(1-W)] \times \sigma_p f_0/f_1$ are plotted as functions of exit projectile energy. The symbols are the same as in Fig. 1. The lines are guides to the eye.

$$\sigma_{10} = \pi R_x^2 [2W(1-W)] , \tag{3}$$

where W is the single-pass vacancy sharing probability.[17] Now these vacancy sharing probabilities for our systems have been measured[14] for gas targets. Thus, we do not need to rely on limited theoretical expressions for finding W.

In this case, we can rewrite (2) as

$$\frac{1}{W(1-W)} \frac{\sigma_{01} f_0}{f_1} = 2\pi R_x^2 + \frac{1}{W(1-W)} \frac{1}{N v \tau} , \tag{4}$$

where we have isolated one term on the right-hand side, $2\pi R_x^2$, as an energy-independent term. In any case, the left-hand side of (4) contains only experimentally measured quantities. Figure 2(b) shows plots of the left-hand side of Eq. (4) as functions of projectile energy for each projectile. It should be noted that for the argon projectiles the relevant vacancies are in the L shell, while for all other projectiles, K-shell vacancies are being discussed. We note that as the energy is increased, these values approach constant values. Furthermore, the deviations from constancy are all now towards increasing the values, consistent with the second term in (4).

The interpretation which emerges is that the steady-state values of the inner-shell vacancy fractions approach a saturation value dictated by the *collisional* mechanisms for vacancy production and vacancy filling. Only at the lower energies does spontaneous decay have a competing role.

As discussed above, the existence of oxygen as an impurity in the carbon foils was established. This causes substantial difficulty in interpreting the oxygen projectile data. While oxygen-carbon cross sections have been measured,[14] oxygen-oxygen cross sections have not, in our energy range. It is expected that the oxygen-oxygen vacancy-filling cross sections should be large, compared to those for carbon-oxygen. Thus we cannot at this time analyze the data for oxygen projectiles in the same fashion. We have carried through an analysis of the effect of the oxygen impurity on the other projectiles, both for vacancy production and vacancy filling. They are found to be negligible at all energies considered here.

From Fig. 2(b) we can read the values of $2\pi R_x^2$. The R_x values are listed in Table I. These values, together with the data from Ref. 14 con-

TABLE I. Geometrical factors.

	B-C	C-C	N-C	Ar-C
R_x(a.u.) [a]	0.83	1.1	1.2	1.2
R_{min} (a.u.)	1.1		1.0	1.7

[a] 1 a.u. = 0.529 Å.

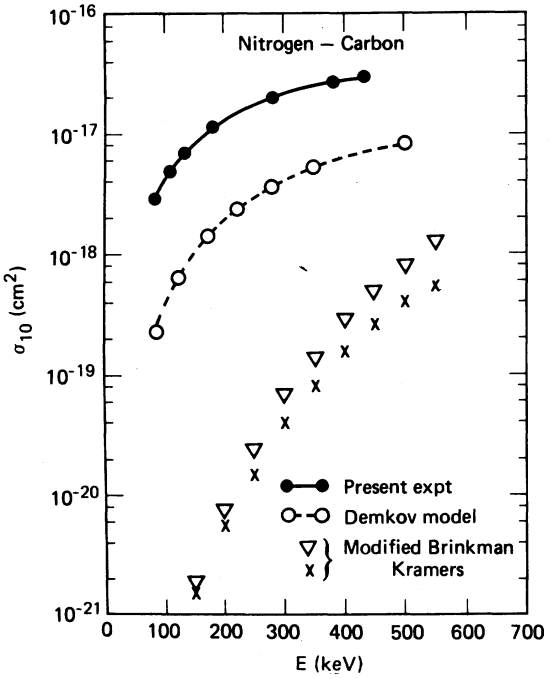

FIG. 3. Cross sections for transfer of vacancies from nitrogen projectiles to carbon atoms: closed circles, present experimental values; open circles, Demkov two-state model; inverted triangles, modified Brinkman-Kramers theory with $Z_1=6$; crosses, modified Brinkman-Kramers theory with $Z_1=7$.

stitute a determination of the charge-transfer cross section for projectile-carbon atom collisions, using Eq. (3).[17] Also listed in that table are the positions of the minima in the 1σ-2σ molecular (3σ-4σ for Ar) orbital energy-difference curves as functions of internuclear distance for the respective systems. These differences were calculated using the variable screening model program of Eichler and Willie,[18] which we have expanded to include a larger basis set.

Figure 3 shows the resultant cross section for the case of nitrogen projectiles. Also shown in the figure are theoretical estimates of the charge-transfer cross section for N-C collisions. It can be seen from the figure that the deduced values of the cross sections are orders of magnitude larger than those predicted by the Brinkman-Kramers theory as modified by Nikolaev[20] and Lapicki and Losonsky.[21] This is due to the quasimolecular nature of the process at these energies and is similar to the effect seen in other inner-shell vacancy production processes when compared to point charged particle theories.[22] As mentioned above, the simple two-state models which take

TABLE II. Lifetimes for K-shell vacancies.

Energy (keV)	τ(sec) B^+	C^+	N^+
100	5.5×10^{-15}	1.5×10^{-15}	4.5×10^{-15}
150	1×10^{-14}	2×10^{-15}	4×10^{-15}
180	1.5×10^{-14}	3×10^{-15}	4×10^{-15}
Theor. ground state lifetime [a]	2×10^{-13}	1.2×10^{-14}	7.5×10^{-15}

[a] From Ref. 19.

the molecular nature of the process into account have been successfully used[15] in interpretation of K-shell vacancy production data. Figure 3 shows our numerical evaluation of the cross section using the Demkov model[16] with α as recommended by Meyerhof.[15] The details of the calculation will be published elsewhere.

The figure shows that the simple two-state quasimolecular theory cross sections are in better agreement with the data than the modified B-K theory. However, other couplings are known to be important[14] and need to be taken into account. This is the reason for our using the experimentally determined single pass probabilities.

Finally, Table II shows the results of solving Eq. (4) for τ at the lower energies where deviations occur in Fig. 2(b). The derived lifetimes are smaller than the theoretical estimates for static ground state configuration vacancies,[19] and are seen to increase with increasing energy. This is an expected result, resulting from outer-shell dynamics.[9] However, the uncertainties associated with these values are large, and assumption dependent.

Further studies of this type are needed to check the assumptions used here. In particular the role of two K-shell vacancies needs to be examined, as does the relevance (or not) of vacancy filling via two-electron processes. Our use of experimental vacancy-sharing probabilities includes these effects, but their roles should be separately understood. This area of investigation promises to be a fruitful source of information about individual inner-shell excitation processes. It is clear that much more theoretical effort is needed to understand the processes involved here.

This work was performed under the auspices of the U.S. Department of Energy by Lawrence Livermore Laboratory under Contract No. W-7405-ENG-48.

*Permanent address: Department of Physics, University of Arizona, Tucson, Ariz. 85721.
[1]N. Bohr and J. Lindhard, K. Dans. Vidensk. Selsk., Mat.-Fys. Med. 28, No. 7 (1954); N. Bohr, Phys. Rev. 58, 654 (1940).
[2]W. E. Lamb, Jr., Phys. Rev. 58, 696 (1940).
[3]H. D. Betz and L. Grodzins, Phys. Rev. Lett. 25, 211 (1970).
[4]H. D. Betz, Rev. Mod. Phys. 44, 465 (1972).
[5]R. J. Fortner and J. D. Garcia, in *Atomic Collisions in Solids*, edited by S. Datz, B. R. Appleton, and C. D. Moak (Plenum, New York, 1975).
[6]H. D. Betz, F. Bell, H. Panke, G. Kalkoffen, M. Welz, and D. Evers, Phys. Rev. Lett. 33, 807 (1974).
[7]R. A. Barragiola, P. Ziem, and N. Stolterfoht, J. Phys. B 9, L447 (1976).
[8]F. Hopkins, J. Sokolov, and A. Little, Phys. Rev. A 15, 588 (1977).
[9]R. J. Fortner and J. D. Garcia, Phys. Rev. A 12, 856 (1975); 19, 2474 (1979).
[10]C. L. Cocke, S. L. Varghese, and B. Curnutte, Phys. Rev. A 15, 874 (1977).
[11]A. R. Knudsen, P. G. Burkhalter, and D. J. Nagel, Phys. Rev. A 10, 2118 (1974).
[12]T. J. Gray, P. Richard, K. A. Jamison, J. M. Hall, and R. K. Gardner, Phys. Rev. A 14, 1333 (1976); T. J. Gray, C. L. Cocke, and R. K. Gardner, *ibid.* 16, 1907 (1977).
[13]S. Datz, B. R. Appleton, J. R. Mowat, R. Laubert, R. S. Peterson, R. S. Thoe, and I. A. Sellin, Phys. Rev. Lett. 33, 733 (1974).
[14]D. Schneider and N. Stolterfoht, Phys. Rev. A 19, 55 (1979); the argon L-shell cross sections are from R. A. Barragiola, P. Ziem, and N. Stolterfoht, J. Phys. B 9, L447 (1976).
[15]W. E. Meyerhof, Phys. Rev. Lett. 31, 1341 (1973); W. E. Meyerhof, R. Anholt, T. K. Saylor, S. M. Lazarus, and L. F. Chase, Jr., Phys. Rev. A 14, 1653 (1976); W. E. Meyerhof, R. Anholt, and T. K. Saylor, Phys. *ibid.* 16, 169 (1977).
[16]Yu. N. Demkov, Zh. Eksp. Teor. Fiz. 45, 195 (1963) [Sov. Phys.—JETP 18, 138 (1964)].
[17]The single-pass vacancy sharing probabilities are given by $W \equiv \sigma_H/(\sigma_H+\sigma_L)$. These cross sections are tabulated in Ref. 14.
[18]J. Eichler and U. Wille, Phys. Rev. Lett. 33, 56 (1974); Phys. Rev. A 11, 1973 (1975).
[19]D. L. Walters and C. P. Bhalla, Phys. Rev. A 3, 1919 (1971). See also E. J. McGuire, in *Atomic Inner Shell Processes I*, edited by B. Craseman (Academic, New York, 1975).
[20]V. S. Nikolaev, Zh. Eksp. Teor. Fiz. 51, 1263 (1966) [Sov. Phys.—JETP 24, 847 (1967)].
[21]G. Lapicki and W. Losonski, Phys. Rev. A 15, 896 (1977); W. Brandt and G. Lapicki, *ibid.* 20, 465 (1979).
[22]See, for example, Figs. 3.22 and 3.26 in J. D. Garcia, R. J. Fortner, and T. M. Kavanagh, Rev. Mod. Phys. 45, 111 (1973).